

Table 2 Parameter estimates from discretized flight data of X-31A unstable aircraft

Parameters	$\partial \dot{q}/\partial \alpha$	$\partial \dot{q}/\partial q$	$\partial \dot{q}/\partial \delta$	$C_{m\alpha}$	C_{mq}	$C_{m\delta}$
Delta	2.539 (0.396) ^a	-1.269 (0.351)	-10.150 (0.851)	—	—	—
Ref. 1	—	—	—	0.119	-1.650	-0.57

^aSample standard deviation.

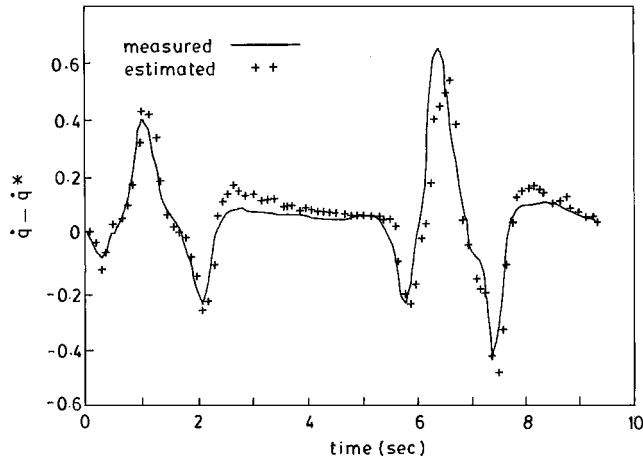


Fig. 1 Comparison of measured and computed accelerations ($\dot{q} - \dot{q}^*$) via the delta method.

denote the trim value of the corresponding variables. This is done to conform results with those reported in Ref. 1. Similarly the output variable is defined as $(\dot{q} - \dot{q}^*)$. The use of $(\dot{q} - \dot{q}^*)$ would also ensure that the assumption made earlier for representing Eq. (3) by Eq. (6) is reasonable, because it implies cancellation of steady-state contributions to pitching moment from the aerodynamic forces and propulsive unit forces.

Once the network is trained, the delta method is used to estimate derivatives $\partial \dot{q}/\partial \alpha$, $\partial \dot{q}/\partial q$, and $\partial \dot{q}/\partial \delta$, and the results are shown in Table 2. The parameter estimates of $C_{m\alpha}$, C_{mq} , and $C_{m\delta}$ from Ref. 1 are also given for ready reference.

Using Table 2, it is readily seen that the ratio $(\partial \dot{q}/\partial \alpha)/(\partial \dot{q}/\partial \delta) = -0.250$ compares reasonably with the ratio $C_{m\alpha}/C_{m\delta} = -0.208$ despite the uncertainties caused by discretization of analog plots of real-flight data and omission of contributions to C_m from the propulsive forces. Next, the estimated derivatives $\partial \dot{q}/\partial \alpha$, $\partial \dot{q}/\partial q$, and $\partial \dot{q}/\partial \delta$ are used to compute the estimated $(\dot{q} - \dot{q}^*) = (\partial \dot{q}/\partial \alpha)\alpha + (\partial \dot{q}/\partial q)q + (\partial \dot{q}/\partial \delta)\delta$. The so-estimated $(\dot{q} - \dot{q}^*)$ shows reasonable match with the actual (discretized) $(\dot{q} - \dot{q}^*)$ as shown in Fig. 1. The discrepancy between the actual and estimated values of $(\dot{q} - \dot{q}^*)$ can be largely assigned to an insufficient number of input variables in the network input file, which, in turn, was caused by a lack of information (for example, about thrust contributions) made available in Ref. 1.

Conclusions

The neural-network-based delta method is shown to be a good alternative to the existing methods for estimating parameters of an unstable aircraft. It does not require postulation of aircraft model, initial guess values of parameters, or estimation of initial conditions. It is a noniterative method and uses the measured flight data directly to train the neural network and subsequently estimate parameters in one go. The applicability of the delta method is shown on simulated as well as discretized analog plots of real-flight data. The results suggest that the delta method can be used advantageously to estimate parameters of an unstable aircraft.

References

- ¹Jategoankar, R. V., and Thielecke, F., "Evaluation of Parameter Estimation Methods for Unstable Aircraft," *Journal of Aircraft*, Vol. 31, No. 3, 1993, pp. 510-519.

²Raisinghani, S. C., Ghosh, A. K., and Kalra, P. K., "Two New Techniques for Aircraft Parameter Estimation Using Neural Networks," *The Aeronautical Journal*, Vol. 102, No. 1011, 1998, pp. 25-29.

³Ghosh, A. K., Raisinghani, S. C., and Khubchandani, S., "Estimation of Aircraft Lateral-Directional Parameters Using Neural Networks," *Journal of Aircraft*, Vol. 35, No. 6, 1998, pp. 876-881.

⁴Waszak, M. R., and Schmidt, D. K., "Flight Dynamics of Aeroelastic Vehicles," *Journal of Aircraft*, Vol. 25, No. 6, 1988, pp. 563-571.

Flight Testing Radar Detection of the Saab 105 in Level Flight

Martin Norsell*

Royal Institute of Technology,
SE-100 44 Stockholm, Sweden

Nomenclature

- G = antenna gain
- k = wave number
- P_{\min} = minimum power level of the received signal necessary for detection
- P_t = transmitted power
- R_d = detection range
- α = angle of attack
- γ = flight-path angle
- λ = wavelength
- ν_0 = radar-dependent detection distance
- σ = radar cross section

Introduction

THE Department of Aeronautics at the Royal Institute of Technology (KTH) has for some time been involved in developing methods for aircraft trajectory optimization. When the developed methods are used, it is possible to compute a flight path taking the aircraft from one state to another in minimum time or using minimum fuel.¹⁻³ The optimized trajectories have been flight tested by the Swedish Air Force using the supersonic Saab J35 Draken² and the jet trainer Saab 105 (Ref. 4).

It is unlikely, in modern combat scenarios, that the optimal flight path with respect to the aircraft performance only is very useful. The main threat against aircraft is radar, which stands for radio detection and ranging. The effectiveness of the radar is determined by range and the geometry of the aircraft. The detection time is defined as the time interval between the instant at which the aircraft is first detected and the instant at which the aircraft reaches the specified target. The detection distance is the distance from the target to the position at which the aircraft is first detected by radar. Given an initial position and a target position, the offset distance is defined as the perpendicular distance to an alternative flight path parallel to the original flight path. Hence, a flight path pointing directly at, or above, the target is defined to have zero offset.

The purpose of the present study is to perform a preliminary investigation of the possibility to reduce the distance to the location where an aircraft is first detected by hostile radar by considering the radar cross section (RCS) properties of the aircraft. To gain understanding of the potential decrease in detection time, a numerical example is considered.

Received 31 January 2002; revision received 3 June 2002; accepted for publication 4 June 2002. Copyright © 2002 by the American Institute of Aeronautics and Astronautics, Inc. All rights reserved. Copies of this paper may be made for personal or internal use, on condition that the copier pay the \$10.00 per-copy fee to the Copyright Clearance Center, Inc., 222 Rosewood Drive, Danvers, MA 01923; include the code 0021-8699/02 \$10.00 in correspondence with the CCC.

*Ph.D. Student, Department of Aeronautics, KTH. Member AIAA.

This Note describes the model and numerical implementation used to calculate the radar detection distance when a Saab 105 approaches a radar station in level flight at different altitudes and with different offset. Trajectory optimization is used to minimize the time a hostile radar has the aircraft under surveillance from point of detection until passing above the radar station. Finally, numerical results together with the results obtained in flight tests are presented and the differences discussed. Improvements for possible future flight tests are also outlined.

Background

If no analytical solution is possible, the current method of choice for exactly solving electromagnetic problems according to Maxwell's equations is the method of moments. Unfortunately, this method is not applicable on large electromagnetic problems such as a full-size aircraft at 10-GHz frequency. This is due to the large, dense, and complex system of equations that needs to be solved.

The calculations of RCS in this Note were performed by Ericsson Microwave Systems (EMW) using physical optics (PO).⁵⁻⁷ The simplification done in PO is to assume that the current at the boundary of the radar-illuminated region is zero. This implies that no currents can follow the shape of the object and interact with other currents at some other boundary. Hence, the PO approximation excludes surface waves. This method becomes more accurate at high frequencies when the wavelength compared to the physical size of the object decreases, and hence, the boundaries become less important.

To avoid radar detection it is only necessary to have sufficiently low RCS, so that the echo returned is below the detection threshold of the radar.⁶ The RCS of a target is a function of the polarization of the incident wave, the angle of incidence, the angle of observation, the geometry of the target, the electrical properties of the target, and the frequency of operation. The backscatter of an object is defined as the equivalent area that would intercept the same amount of incident power to produce the same scatter power density at the receiver site if the object scattered uniformly in all directions.⁸ A simple form of the basic radar range equation is given by⁹

$$R_d^4 = \frac{P_t G^2 \lambda^2 \sigma}{(4\pi)^3 P_{\min}} \quad (1)$$

Equation (1) can be split into two separate parts, one radar dependent and another that is the aircraft RCS, giving

$$R_d = v_0 \sigma^{\frac{1}{4}} \quad (2)$$

The aircraft RCS depends on the orientation of the aircraft relative to the radar station. An airplane in normal flight experiences vibrations due to perturbations such as turbulence in the surrounding air. This affects the RCS seen by the detecting radar. Because the RCS can vary several orders of magnitude for very small variations in angle, this effect may have significant influence on the RCS and, hence, the detection distance.

Numerical Simulation

Approximate RCS data for the Saab 105 was obtained from EMW. The canopy of the Saab 105 is not treated to be reflective and, hence, excluded from the analysis. Furthermore, the fences on the wing are not modeled. These are placed at 90-deg angle to the wing and contribute to the overall RCS as dihedrals, which are known to give large RCS contribution.⁵ The data are given for 0 to -10 deg in elevation and for 0 to 99.75 deg in azimuth. The resolution is 1 deg in elevation and 0.2 deg in azimuth.

The case implemented uses radar data for EMW's HARD radar, equipped with a prototype antenna. HARD is a small three-dimensional tracking and guidance radar for anti-aircraft defense. Because of its randomness, detection performance is usually stated in terms of probabilities. The most commonly used is the blip-scan ratio. It is the probability of detecting a given target at a given range and altitude anytime the antenna beam scans across the target.¹⁰ The detection probability for the HARD radar using the prototype

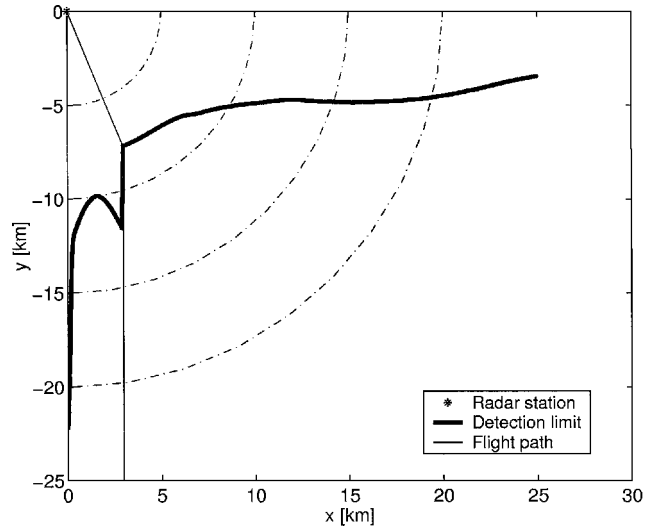


Fig. 1 Optimized flight path in the xy plane, altitude fixed at 850 m.

antenna is given to be 0.8 for a target with $\sigma = 1 \text{ m}^2$, but is not further specified. Because of the limited coverage in elevation of the RCS data available, the lower and upper altitude limits are fixed at 0.1 and 1.2 km, respectively, thus also avoiding the reflective contribution present for angles less than 0.1 deg above the radar horizon. Straight and level flight with $\gamma = 0$ until the detection distance is assumed. When the aircraft is detected, the optimal flight path with respect to detection time is calculated and used in the evaluation.

Furthermore, the aircraft is assumed to pass above the radar station at 1-km altitude. If the initial altitude is held constant, the result shown in Fig. 1 is obtained. The altitude is fixed at 850 m, the radar station is placed in the origin, and the detection limit is shown to vary as a function of the initial offset. The RCS of the aircraft depends on both the azimuth and elevation toward the radar station. When the aircraft approaches the radar station in level flight with some offset, the azimuth and elevation both change continuously. This is the primary cause for the local minima and discontinuities shown in the detection limit in Fig. 1, although the underlying RCS representation is smooth. Most conventional airplanes have high RCS straight ahead due to the large radar reflections caused by the engine intakes. This is the reason for the long detection distance when approaching the radar station head on. If the radar station is simply approached with some initial offset, the detection distance can be reduced by more than 50%. For optimization purposes, the many local minima provides a challenging task and will be subject to further research.

When the three-dimensional problem is considered looking at all combinations of the x - y and y -altitude plots, many local minima are detected. It can be concluded that even if the globally optimal flight path is not found, substantial reductions in detection time can be achieved.

The results from this simple example show that the detection time can be significantly reduced. The detection time if approaching the radar straight on at minimum altitude, 100 m, is 108 s. If the aircraft approaches the radar with an initial offset of 4.35 km and at an altitude of 1150 m, the detection time is 40.5 s, a reduction of more than 60%.

Flight Testing

Based on the numerical results, the main concern is to check if it is possible in practice to reduce the detection distance and the corresponding detection time by simply flying off to the radar station. It is also valuable to get an indication of the statistical measure most appropriate to describe the RCS of the aircraft.

The radar used in the test is the HARD radar manufactured by EMW. It is an X-band radar that uses an instrumented range of

20 km, that is, the radar is limited to only consider radar echoes inside that range. In the test, 12 discrete frequencies in the 9-GHz range are used. Furthermore, a prototype antenna with well-defined properties is used.

The approximate RCS used for comparison with the flight-test results is available for 80 discrete frequencies in the 9.6-GHz range. The difference between the frequency used in the measurements and calculations affects the detection distance. When Eq. (1) is examined and it is known that $\sigma = \sigma(\lambda)$, the effect on the detection distance can be divided into two separate parts.⁶ First, the wave number can be calculated $k \equiv 2\pi/\lambda \approx 188 \text{ m}^{-1}$. Together with the physical dimensions of the aircraft, this is well into the high-frequency region suitable for PO calculations. In this region, collective interactions are very weak so that the body is treated as a collection of independent scattering points.¹¹ The net scattering is the complex phasor sum of all of the isolated points. Hence, the RCS is approximately equal to the projected geometrical area if multiple reflection, diffraction, and similar parameters are neglected.

Second, when the detection range and v_0 in Eq. (2) are considered, it can be concluded that

$$\frac{v_{0\text{calc}}}{v_{0\text{measured}}} = \left(\frac{\lambda_{\text{calc}}}{\lambda_{\text{measured}}} \right)^{\frac{1}{2}} \quad (3)$$

Hence, the total error between the calculated detection range and the measured detection range is about 3%, if multiple reflection, diffraction, and similar parameters are neglected. The detection probability used throughout the calculations is 0.8.

The geographical coordinates obtained from the global positioning system (GPS) receivers are differentially corrected using the methods outlined by Wanvik¹² and transformed into Cartesian coordinates with the radar station placed at the origin for convenient visualization.

The coordinate system used in the RCS calculations is the same as the coordinate system used for aerodata calculations. The latter is the basis for the Saab 105 six-degree-of-freedom model used for calculating α , for each test case.⁴ This effect is accounted for to calculate the correct elevation and azimuth angle for the body-fixed RCS coordinate system. The difference experienced in α is between 1.1 and 0.65 deg depending on altitude and remaining fuel. This does not have any significant effect on the calculated RCS, but this is probably due to the low resolution, 1 deg, in elevation. The indicated airspeed used throughout the tests is 500 km/h to avoid any low Doppler effects when flying at large offset distance with respect to the target. All calculations are based on the assumption of level flight, $\gamma = 0$.

A total of 16 test cases were conducted during 2 flights. All tests were performed with the same aircraft, E40. The aircraft was equipped with GPS for data logging and time reference. The pressure altitude in the aircraft was used for altitude determination throughout the tests. The weather was good during both flights with little or no wind. In Fig. 2, a typical test case is shown. The radar station is placed at the origin and approached head on. The altitude is 400 m, and the flight path is represented by the dot-dashed line. The flight path shown in Fig. 2a is the same as the one shown in Fig. 2b, but all of the different curves are shown separately. The time $t = 0 \text{ s}$ is defined as the place where the test case is started. In this particular case, the calculations showed that the aircraft should be detected after approximately 90-s flight time. The first time the tracking function of the radar is initiated does not occur until after 105 s. Furthermore, the radar is seen to lose track and not lock onto the aircraft firmly until about 140 s into the test case. A complete overview of all of the test cases is shown in Table 1.

The RCS used in the calculations is the maximum over the 80 frequencies calculated. The ongoing debate about using mean- or median-valued RCS does not apply here because the HARD radar measures 12 discrete frequencies and uses the best information available. Other statistical measures have been used, resulting in larger differences than what is presented in this Note. For some test cases, the difference in the calculated and actual detection distance is over 3 km. These differences are believed to be caused mainly by

Table 1 Detection distance in flight test compared to numerical results

Test	Pressure altitude, m	Offset, km	Detection distance		
			Calculated, km	Measured, km	Error, %
1	550	0.0	14.8	13.4	+10.6
2	550	2.5	16.2	14.7	+10.3
3	850	0.0	14.1	15.6	-9.3
4	850	2.5	14.0	14.7	-5.0
5	1150	0.0	13.1	13.8	-4.9
6	1150	2.5	14.4	11.4	+26.0
7	550	0.0	14.0	16.7	-15.7
8	550	2.5	16.0	16.5	-2.7
9	550	4.0	15.1	17.0	-10.6
10	700	0.0	22.0	18.9	+16.6
11	700	2.5	14.6	16.1	-9.2
12	700	4.0	15.5	15.6	-0.9
13	850	0.0	19.6	19.2	+2.3
14	850	2.5	12.8	12.2	+5.7
15	850	4.0	17.2	17.3	-0.1
16	400	0.0	23.7	19.8	+19.9

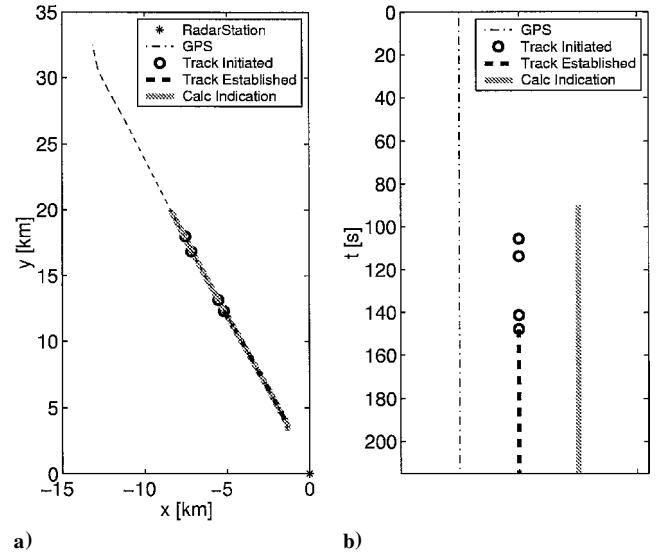


Fig. 2 Approaching the radar station at 400-m altitude head on.

the RCS modeling. The RCS calculations are performed using PO, which excludes multiple reflections, diffraction and similar parameters. RCS calculations of full-size aircraft using more exact methods are known to be very cumbersome, if at all possible.⁶ Furthermore, the RCS may change several orders of magnitude for small angular changes, which can effect the results. Hence, for future tests refined attitude determination is suggested.

In Fig. 3, all of the tests performed at 850-m altitude are shown. The radar station is approached head on, 2.5 and 4.0 km offset. When the detection distance along each test case is examined, it can be concluded that by approaching the radar station with some offset the detection distance and detection time can be substantially decreased. The detection limit shown in Fig. 1 predicts this behavior. Note that the radar starts to track the aircraft and then loses the track again, several times during the test cases. This may be possible to avoid by small course changes if the RCS modeling is improved and optimization methods are developed.

Finally, the maximum detection distance experienced in the flight test was 19.8 km when approaching the radar station head on at 400-m altitude. The shortest detection distance during the tests was 11.4 km, when approaching 2.5 km offset to the radar station at 1150-m altitude, a reduction of more than 40%. The flight time from these two states, with the optimal flight path with respect to minimum time, is calculated using the method described by Ringertz.⁴

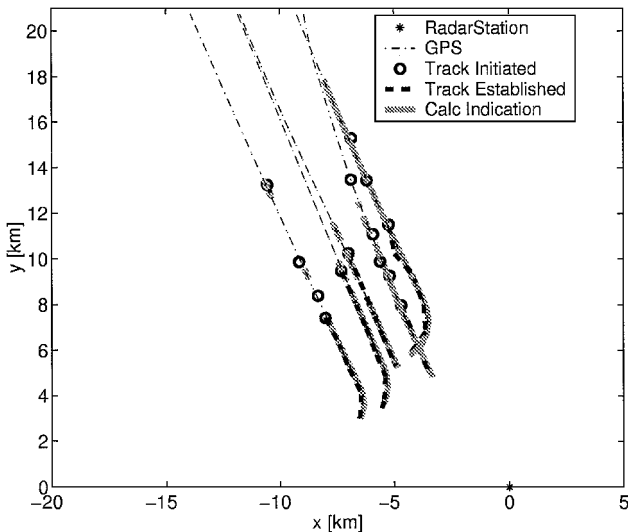


Fig. 3 Approaching the radar station at 850-m altitude.

Passing the radar station at 1000-m altitude results in flight times of 106 s and 60 s, respectively, which corresponds to a reduction of 43% in detection time. Hence, the reduction in the calculated detection time is possible to obtain in reality. This is achieved without any optimization methods applied.

Conclusions

The most important conclusion from the flight test is that substantial decrease in the time interval between the instant at which the aircraft is first detected by hostile radar and the instant at which the aircraft reaches a specified target is possible.

The current test suggests that the maximum RCS value over all radar frequencies should be used. To utilize successfully the computational models of RCS and radars, these models have to be updated and further verified, alternatively using measured data only. It may be possible to use a spline representation of the RCS for future use in optimization.

The example considering a Saab 105 in level flight approaching a radar station shows a reduction in detection time by almost 50%. The results in the flight tests show a difference in the detection time of 40%. This is obtained without optimization methods and shows the great potential in using flight-path optimization with radar range constraints. Future work will include a more general optimization formulation, where the radar range constraints are part of the trajectory optimization problem.

Acknowledgments

This project is financially supported by the Swedish Defence Materiel Administration monitored by Curt Eidefeldt, Staffan Lundin, Björn Jonsson, Bertil Brännström, Jenni Nylander, and Måns Bergmark. The author would also like to thank Mats Henningsson, Kjell Petterson, and Claes-Göran Edström of F10 Air Force Base in Ängelholm. The support of Kerstin Fredriksson, Anders Höök, Henrik Hallenberg, and Kent Johansson of Ericsson Microwave Systems are gratefully acknowledged.

References

- Ringertz, U. T., "Aircraft Trajectory Optimization as a Wireless Internet Application," Dept. of Aeronautics, TR 2000-11, Royal Inst. of Technology, Stockholm, Aug. 2000.
- Ringertz, U. T., "Flight Testing an Optimal Trajectory for the Saab J35 Draken," *Journal of Aircraft*, Vol. 37, No. 1, 2000, pp. 187–189.
- Ringertz, U. T., "Optimal Trajectory for a Minimum Fuel Turn," *Journal of Aircraft*, Vol. 37, No. 5, 2000, pp. 932–934.
- Ringertz, U. T., "Multistage Trajectory Optimization Using Large-Scale Nonlinear Programming," Dept. of Aeronautics, TR 99-25, Royal Inst. of Technology, Stockholm, Sept. 1999.
- Balanis, C., *Antenna Theory Analysis and Design*, Wiley, 1997, pp. 90–98.

⁶Jenn, D., *Radar and Laser Cross Section Engineering*, AIAA Educational Series, AIAA, Washington, DC, 1995, Chaps. 1–2.

⁷Diaz, L., and Milligan, T., *Antenna Engineering Using Physical Optics, Practical CAD Techniques and Software*, Artech House, Norwood, MA, 1996, Chaps. 1, 7.

⁸Cheng, D., *Field and Wave Electromagnetics*, Addison Wesley Longman, Reading, MA, 1989, pp. 637–642.

⁹Paterson, J., "Overview of Low Observable Technology and Its Effects on Combat Aircraft Survivability," *Journal of Aircraft*, Vol. 36, No. 2, 1999, pp. 380–388.

¹⁰Stimson, G., *Introduction to Airborne Radar*, 2nd ed., Scitech, Mendham, NJ, 1998, Chap. 10.

¹¹Knott, E., Shaeffer, J., and Tuley, M., *Radar Cross Section*, 2nd ed., Artech House, Norwood, MA, 1993, Chap. 5.

¹²Wanvik, V., "GPS Based Flight Mission Evaluation," M.S. Thesis 99-07, Dept. of Aeronautics, Royal Inst. of Technology, Stockholm, April 1999.

Maximum Steady Roll Rate in Zero-Sideslip Roll Maneuvers of Aircraft

Nandan K. Sinha* and N. Ananthkrishnan†
Indian Institute of Technology, Bombay,
Mumbai 400076, India

I. Introduction

THE maximum steady roll rate achievable in response to an aileron input, in a maneuver where the sideslip is constrained to be zero, is a useful design parameter for combat aircraft. A larger value of the maximum roll rate, especially over the range of combat Mach numbers, is generally considered to be indicative of superior roll performance.¹ In practice, the zero sideslip constraint is implemented by using an aileron–rudder–interconnect law that suitably schedules the rudder as a function of the aileron deflection. It is commonly believed that the maximum achievable roll rate is limited by lack of aileron control power, or because the zero sideslip constraint cannot be enforced due to limits on the rudder deflection, or due to structural constraints.² However, for modern high-performance aircraft, nonlinear effects due to kinematic and inertial coupling (commonly called roll coupling) are dominant, and the maximum steady roll rate is usually decided by dynamic stability considerations. The purpose of this Note is to illustrate how the maximum steady roll rate in a zero-sideslip roll maneuver, in the presence of roll coupling nonlinearities, may be calculated using a continuation algorithm.

The problem of instabilities in rapid roll maneuvers of aircraft has been widely discussed in the literature ever since the phenomenon of roll coupling was first discovered by Phillips³ in 1948. Hacker and Oprisiu⁴ provided a review of the roll coupling problem, Schy and Hannah⁵ interpreted the instability as a jump phenomenon, Carroll and Mehra⁶ introduced the use of bifurcation analysis for prediction of roll-coupled instability, Jahnke and Culick⁷ applied bifurcation theory to compute points of onset of instability for the F-14, and Ananthkrishnan and Sudhakar⁸ suggested strategies to prevent jump in roll-coupled maneuvers. More recently, Goman et al.⁹ have reviewed the use of bifurcation methods for nonlinear flight dynamics

Received 16 May 2002; revision received 24 June 2002; accepted for publication 25 June 2002. Copyright © 2002 by the American Institute of Aeronautics and Astronautics, Inc. All rights reserved. Copies of this paper may be made for personal or internal use, on condition that the copier pay the \$10.00 per-copy fee to the Copyright Clearance Center, Inc., 222 Rosewood Drive, Danvers, MA 01923; include the code 0021-8669/02 \$10.00 in correspondence with the CCC.

*Ph.D. Student, Department of Aerospace Engineering; nandan@aero.iitb.ac.in.

†Assistant Professor, Department of Aerospace Engineering; akn@aero.iitb.ac.in. Senior Member AIAA.